European Journal of Pharmaceutical Sciences 46 (2012) 167–172

Contents lists available at SciVerse ScienceDirect

European Journal of Pharmaceutical Sciences

journal homepage: www.elsevier.com/locate/ejps

Conjugation of paclitaxel on adeno-associated virus (AAV) nanoparticles for co-delivery of genes and drugs

Fang Wei [a], Kellie I. McConnell [a], Tse-Kuan Yu [b], Junghae Suh [a,*]

[a] Department of Bioengineering, Rice University, Houston, Texas, USA
[b] Department of Radiation Oncology, The University of Texas M.D. Anderson Cancer Center, Houston, Texas, USA

ARTICLE INFO

Article history:
Received 17 October 2011
Received in revised form 22 February 2012
Accepted 26 February 2012
Available online 3 March 2012

Keywords:
Taxol
Drug delivery
Gene delivery
Immunoblotting
Fluorescence microscopy
Cytotoxicity

ABSTRACT

We have investigated the use of adeno-associated virus (AAV) nanoparticles as platforms for the co-delivery of genes and drugs to cancer cells. With its regular geometry, nanoscale dimensions, lack of pathogenicity, and high infection efficiency in a wide range of human cells and tissues, AAV is a promising vector for such applications. We tested the covalent conjugation of paclitaxel onto surface-exposed lysine residues present on the virus capsid. Immunoblotting results suggest successful attachment of drug molecules to the virus nanoparticles. Favorably, the reaction conditions did not reduce the gene delivery efficiency of the AAV vectors. Unfortunately, decrease in cancer cell viability was not observed with our AAV–taxol conjugates. For future attempts at conjugating drugs to the AAV nanoparticle, we have identified several improvements than can be considered to achieve the desired cytotoxicity in target cells.

1. Introduction

A number of virus capsid-based nanoparticles are currently being investigated as drug delivery platforms (Franzen and Lommel, 2009; Hughes, 2005; Manchester and Singh, 2006; Steinmetz, 2010; Yoo et al., 2011). For example, the chemotherapeutic drug paclitaxel (or taxol) has been covalently attached to the capsid of bacteriophage MS2 through cysteine alkylation (Wu et al., 2009). The virus capsid scaffold helped to increase the solubility of taxol while maintaining similar cytotoxicity levels as free drug. Several types of plant viruses have also been tested as drug delivery platforms (Loo et al., 2008; Ren et al., 2007). An advantage of using bacteriophage or plant viruses for drug delivery applications is the ability to obtain large quantities of virus material readily. Unfortunately, these viruses are ineffective at delivering genes to human cells, so therapeutic approaches desiring to co-deliver drugs and genes via these delivery vectors may require substantial re-engineering of the viruses to achieve target efficacies. To overcome this problem, mammalian viruses can be used as alternatives for applications requiring co-delivery of drugs and genes.

Adeno-associated virus (AAV) is a promising mammalian virus vector commonly used for gene therapy applications (Mueller and Flotte, 2008). It is considered to be one of the safest viral vectors due to its nonpathogenic nature and limited immunogenicity. AAV is a non-enveloped virus with a single-stranded DNA genome that contains two genes: *rep* and *cap*. The virus capsid, 25 nm in diameter, is composed of 60 subunits: VP1, VP2, and VP3 assembled in a 1:1:10 ratio (Grieger and Samulski, 2005). The supramolecular capsid assembly lends itself well to multivalent conjugation of small molecules. Therefore, with its regular geometry, nanoscale dimensions, lack of pathogenicity, and high infection efficiency in a wide range of human cells and tissues, AAV is a highly promising vector for biomedical applications requiring co-delivery of small molecules and genes.

Thus far, small molecule drugs have not been conjugated to the AAV capsid so it is unclear if AAV will be amenable for co-delivery of drugs and genes from the same platform. Co-administration of drugs and AAV (i.e. mixing drugs and AAV vectors in the same injection without use of covalent conjugation) has been tested by others (Hillgenberg et al., 1999; Jiang et al., 2011; Koppold et al., 2006; Zhang et al., 2010). Interestingly, chemotherapeutic drugs appear to increase gene delivery efficiencies of AAV vectors under certain conditions through unknown mechanisms.

In this study, we investigate the covalent conjugation of taxol as a model drug onto the AAV scaffold. Taxol was first converted to taxol-NHS ester and then conjugated to the approximately 300 surface-exposed lysine residues on the AAV capsid (Fig. 1). Results indicate the conjugation reaction does not adversely impact gene delivery or cytotoxicity of the virus nanoparticles.

* Corresponding author. Address: 6100 Main Street, Houston, Texas 77005, USA. Tel.: +1 713 348 2853; fax: +1 713 348 5877.
E-mail address: jsuh@rice.edu (J. Suh).

0928-0987/$ - see front matter © 2012 Elsevier B.V. All rights reserved.
doi:10.1016/j.ejps.2012.02.022

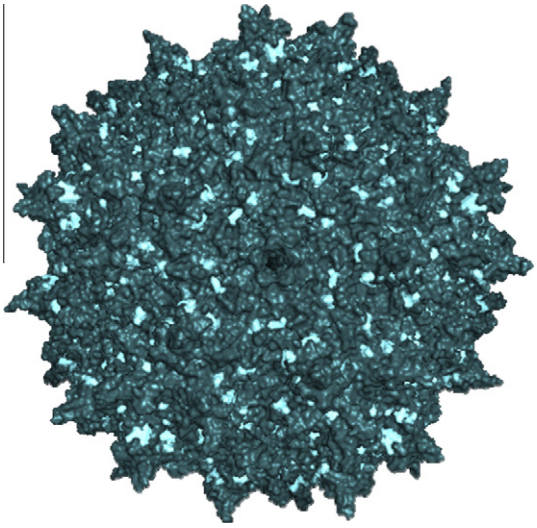

Fig. 1. Surface-exposed lysines on AAV capsid. Approximately 300 of the 1080 lysine residues per virus capsid are surface-exposed (light blue). Surface-exposed lysines were determined using VIPERdb, based on residue radius and solvent accessible surface area (5 lysines per subunit × 60 virus subunits per capsid). Image generated by Pymol. (For interpretation of the references to color in this figure legend, the reader is referred to the web version of this article.)

2. Methods

2.1. Synthesis of taxol-NHS ester

The synthesis followed a published procedure by Luo and Prestwich (1999). Briefly, dry pyridine (10-fold molar excess) was added to a stirring solution of taxol (LC laboratories) and succinic anhydride (1.2 equivalents) in dichloromethane at room temperature. The reaction mixture was stirred for 3 days at room temperature and then concentrated in a rotary evaporator. The residue was dissolved in dichloromethane, and taxol-2′-hemisuccinate was purified by recrystallization with water. Mass calculated for $C_{51}H_{55}NO_{17}$: 953.99. Found: $[M]^+$: 954.1, $[M+Na]^+$: 977, $[M+K]^+$: 992.7 (Fig. S1).

Next, *N*-hydroxysuccinimido diphenyl phosphate (SDPP) was prepared from diphenylphosphoryl chloride, *N*-hydroxysuccinimide, and triethylamine in dichloromethane as previously described (Ogura et al., 1980). Crude SDPP was washed with ether, dissolved in ethyl acetate, washed with water, dried with magnesium sulfate, and concentrated in vacuo. Triethylamine (4 equivalents) was added to a solution of taxol-2′-succinate and SDPP (1.5 equivalents) in acetonitrile. The reaction was stirred for 6 h at room temperature and then concentrated in vacuo. The residue was dissolved in ethyl acetate and hexane and purified on silica gel. Thin Layer Chromatography (TLC) showed R_f of 0.52. Mass calculated for $C_{55}H_{58}N_2O_{19}$: 1051.07. Found: $[M]^+$: 1050.9, $[M+Na]^+$: 1073.6, $[M+K]^+$: 1089.7 (Fig. S2).

2.2. Virus production

Virus was produced as described elsewhere (Xiao et al., 1998). Briefly, pXX2 (AAV2 *rep* and *cap* genes) and AV-GFP (CMV promoter and GFP gene between viral ITRs) were transfected with pXX6 (adenoviral helper genes) into HEK 293T cells using polyethylenimine. All three plasmids were generously provided by Dr. R. Jude Samulski (University of North Carolina at Chapel Hill). Virus was separated using ultracentrifugation and an iodixanol step gradient. Virus iodixanol solution was further purified by using HiTrap Heparin HP columns (GE Healthcare). The column was loaded with 1 ml virus iodixanol solution, washed with 10 mM Tris buffer and eluted with Tris buffer with high NaCl concentrations (1 M). Elution was dialyzed against 10 mM sodium phosphate buffer using slide-a-lyzer dialysis cassette (Pierce) with a MWCO of 10 kD. Titers were determined by quantitative real-time PCR (QPCR) using SYBR Green PCR Master Mix (Applied Biosystems, Foster City, CA) with primers against the CMV promoter. For this study, the recombinant AAV vector encoding GFP is called "wtAAV" to indicate the capsid is wildtype.

2.3. AAV–taxol conjugations

Taxol-NHS ester dissolved in DMSO was added to AAV2 virus in DPBS (10 mM sodium phosphate, 300 mM NaCl) at a molar ratio of 100 k taxol-NHS per virus capsid. The final concentration of DMSO is less than 10% to ensure homogeneity of the solution. The reaction was protected from light and rocked for over 12 h at 4 °C. The mixture was transferred to a dialysis cassette (Piece, 10 kD cutoff) and dialyzed against acetone:DPBS (50:50) for 1 h and then dialyzed against three buffer exchanges of DPBS only. For this study, the recombinant AAV vector encoding GFP and conjugated with taxol is called "AAV–taxol".

2.4. Western blots

Western blots were performed by denaturing virus in NuPAGE LDS buffer (Invitrogen, Carlsbad, CA) for 10 min at 70 °C. Samples were loaded on NuPAGE 7% Tris–acetate gels (Invitrogen) and run for 90 min. Samples were transferred to Hybond ECL nitrocellulose membrane (GE Healthcare, Piscataway, NJ) and blocked using 5% skim milk in PBS-T (137 mM NaCl, 2.7 mM KCl, 10 mM Na_2HPO_4, 2 mM KH_2PO_4, 0.1% Tween-20). Membranes were either incubated for 1 h with B1 antibody (American Research Products, Belmont MA) or anti-taxol antibody (Santa Cruz Biotechnology, Santa Cruz, CA), each at a 1:50 dilution in PBS-T. Samples were rinsed with PBS-T and incubated with a 1:2000 dilution of HRP-conjugated goat anti-mouse secondary antibody for 1 h (Jackson Immunoresearch, West Grove, PA). Samples were rinsed with PBS-T and incubated with Lumi-Light Western blotting substrate (Roche Diagnostics, Indianapolis, IN). Samples were then digitally imaged using a FluorChem FC2 imager.

2.5. Dot blots

Dot blots were performed by diluting virus in PBS (137 mM NaCl, 2.7 mM KCl,10 mM Na_2HPO_4, 2 mM KH_2PO_4) and then applying the virus samples to a Bio-Dot microfiltration apparatus (Bio-Rad, Hercules, CA). Membranes were blocked as for Western blotting and incubated with A20, A1, B1, or anti-taxol antibodies (1:200 dilutions). Secondary antibody application and visualization were performed as with Western blots.

2.6. Transmission electron microscopy (TEM)

5–10 μl of wtAAV or AAV–taxol samples were applied to continuous carbon-coated copper grids (Ted Pella) and stained with freshly prepared 0.75% uranyl formate solution. JOEL 2010 electron microscope operating at 120 kV was used to image the samples.

2.7. Gene expression analysis

HeLa cells were seeded on glass coverslips in 24 well plates such that cell confluency would reach 75% at 24 h post seeding. Virus samples (both unconjugated AAV and AAV–taxol) were applied at an MOI of 10,000 in duplicate wells in 200 μL complete media. Additional media (1 ml complete media) was added 4 h

post-infection. After 48 h, samples were fixed with 4% paraformaldehyde in PBS and mounted onto glass slides. Samples were imaged using a Zeiss LSM 5 LIVE confocal microscope.

2.8. MTT viability assay

HeLa cells were plated so that cell density would be 40-50% at 24 h post seeding. Virus (wtAAV2 and AAV2-taxol) was added at an MOI of 50,000. Three days later, media was removed and MTT (5 mg/ml, Sigma Aldrich) was added in a 1:2 ratio with fresh media. Three hours later, media was removed and samples were dissolved in 250 μL DMSO. For each sample, the absorbance was measured at 570 nm using a Magellen plate reader.

3. Results and discussion

3.1. Synthesis of AAV–taxol conjugates

Taxol was chemically modified in preparation for conjugation to the approximately 300 surface exposed lysine residues on the AAV capsid (Fig. 1). Chemically modifying the hydroxyl group at position 2′ and 7 does not affect the drug potency (Deutsch et al., 1989; Lataste et al., 1984; Parness et al., 1982). Due to steric effects, hydroxyl groups at the 1 and 7 positions are not as active as hydroxyl group at the 2′ position (Fig. 2) (Deutsch et al., 1989; Magri and Kingston, 1986; Mathew et al., 1992). Because of this, we have chosen to modify the hydroxyl group at the 2′ position. An ester bond was used to create a succinic linker, which was then converted to an NHS ester for conjugation to AAV. Ester bonds are known to easily hydrolyze in weak basic or acid conditions (Dosio et al., 1997). Once an AAV–taxol conjugate enters a cell, the weakly acidic conditions should induce the breakage of the ester bond, releasing taxol molecules into the cell. Our AAV–taxol conjugates were created through three synthesis steps (Fig. 2). First, taxol was converted into 2′-taxol succinate following a previously published method (Luo and Prestwich, 1999). The mass of the product was confirmed by mass spectrometry (Fig. S1). Then, SDPP was reacted with 2′-taxol succinate to form taxol-NHS ester. The final product was purified by column chromatography and taxol-NHS ester mass was confirmed by mass spectrometry (Fig. S2). Finally, taxol-NHS in DMSO was conjugated to AAV capsids in DPBS buffer. The un-reacted taxol was removed by dialysis against 50% acetone/DPBS, as dialysis with DPBS alone was unsuccessful in removing free taxol (data not shown).

3.2. Dialysis against 50% acetone in DPBS does not affect capsid structure

Fifty percent acetone in water has been used previously to purify macromolecules conjugated to taxol (Luo and Prestwich, 1999; Luo et al., 2000). We evaluated the effects of exposure to 50% acetone on virus capsid stability. One batch of virus was divided into

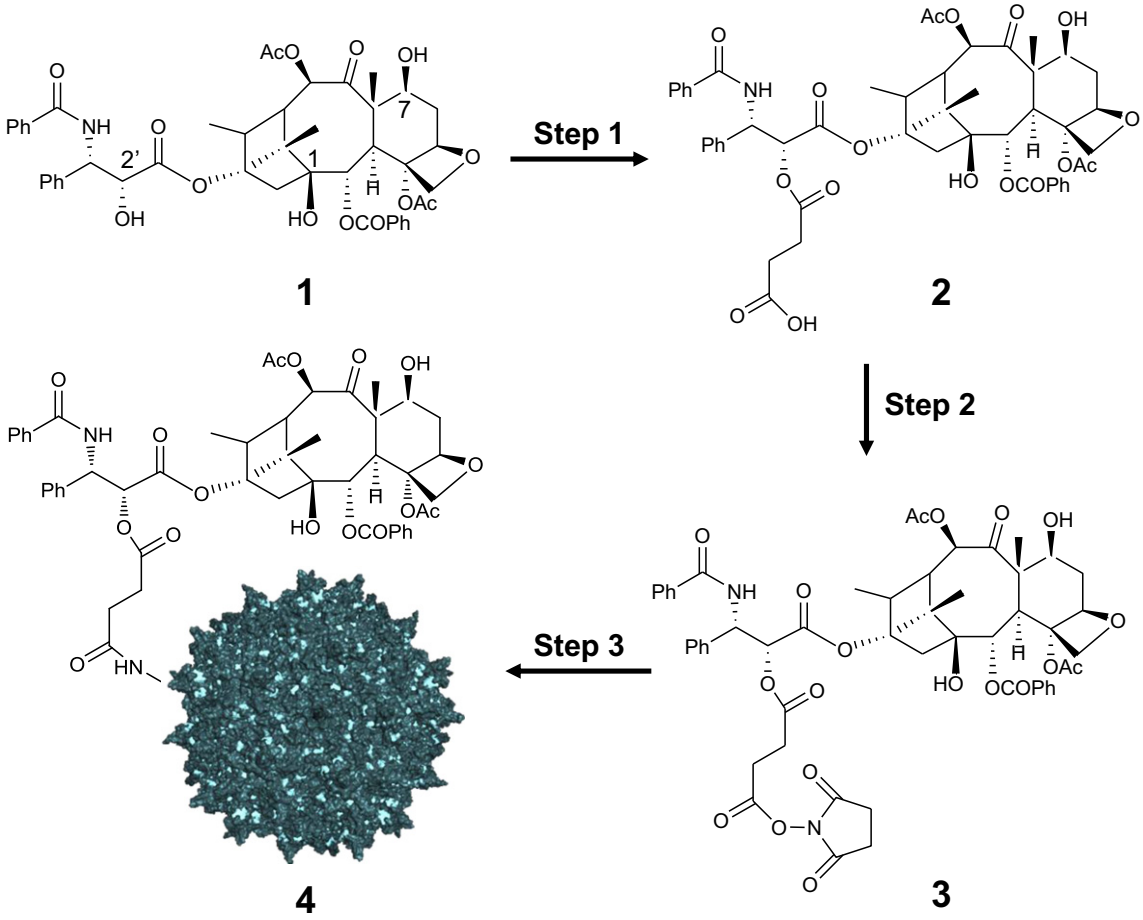

Fig. 2. Synthesis of AAV–taxol. Step 1: succinic anhydride was added to taxol (1) in dichloromethane, pyridine was then added into the reaction, and the reaction was kept at room temperature for 3 days to form 2′-taxol succinate (2). Step 2: SDPP was added to 2′-taxol succinate in acetonitrile, triethylamine was then added, and the reaction was kept at room temperature for 3 h to form taxol-NHS ester (3). Step 3: Taxol-NHS ester in DMSO was added to DBPS containing AAV nanoparticles. The reaction was kept at 4 °C overnight to form AAV–taxol (4). SDPP: *N*-hydroxy-succinimido diphenyl phosphate. DMSO: Dimethyl Sulfoxide. DPBS: Dulbecco's Phosphate Buffered Saline.

two portions – one portion was dialyzed against 50% acetone/water and the other portion was dialyzed against 50% acetone/DPBS. Dialysis solution was changed after 1 h followed by three additional changes in DPBS. Dot blot analysis was used to evaluate the integrity of the virus capsid after dialysis. Three antibodies were used to characterize the capsid: A20 (binds to only intact virus capsids), A1 (binds the N-terminus of VP1, inaccessible for intact capsids), and B1 (binds C-terminus of all three VPs and is only accessible when capsid has been denatured). Dot blot staining (Fig. S3) indicates that AAV capsids remain intact after dialysis against 50% acetone in both DPBS and water. This is suggested by positive A20 staining and the absence of A1 or B1 staining (detected in denatured virus). Because virus dialyzed against 50% acetone/water began to aggregate after 1 h, 50% acetone/DPBS was used as dialysis solvent for removal of un-reacted taxol-NHS ester. Overall, dialysis of AAV against 50% acetone in DPBS does not adversely impact capsid stability.

3.3. Confirmation of successful AAV–taxol conjugation

Dot blot analysis was performed to verify the successful conjugation of taxol-NHS onto AAV capsids (Fig. 3). Positive A20 staining for AAV–taxol conjugate indicates that AAV capsids remain intact after undergoing the reaction and subsequent dialysis against 50% acetone in DPBS. Notably, positive α-taxol staining indicates the presence of taxol on the conjugated virus capsids. Mock conjugation reactions were performed to ensure the complete removal of free taxol-NHS after 50% acetone/DPBS dialysis. These conjugations were performed as an exact parallel to the AAV–taxol conjugation, but without the addition of virus. A lack of positive α-taxol staining for the dialyzed taxol-NHS control indicates that our 50% acetone/DPBS dialysis protocol is successful for removing all free taxol.

Western blot analysis was performed to further confirm the successful conjugation of taxol to the AAV capsid (Fig. 4). B1 antibody was used to detect the common C-terminus of the three capsid proteins: VP1, VP2 and VP3. As subunits are incorporated into the AAV capsid in a 1:1:10 ratio (VP1:VP2:VP3), we observe a more intense VP3 band as compared to VP1 and VP2. Both wtAAV and AAV–taxol conjugations yield similar B1 staining (Fig. 3, left). An anti-taxol antibody was used to detect the presence of taxol conjugated on the AAV capsid subunits. As shown in Fig. 4 (right), unconjugated wtAAV capsid does not yield positive taxol staining. However, AAV–taxol conjugate shows positive anti-taxol staining at the correct molecular weights of VP1, VP2, and VP3, suggesting successful conjugation of taxol onto the AAV capsid.

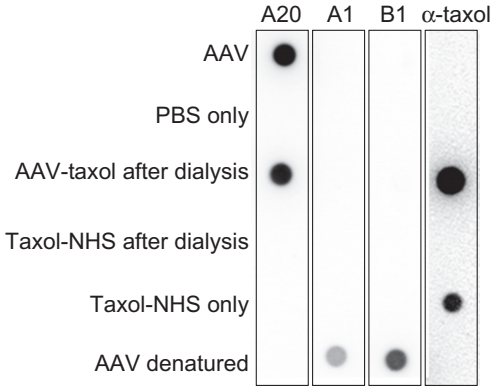

Fig. 3. Dot blot of AAV–taxol conjugates show successful conjugation of taxol to intact virus capsids. Four antibodies were used to characterize the capsid: A20 binds intact virus capsids, A1 binds N-terminus of VP1 (for capsids that have been activated by temperature shock (Musick et al., 2011)), B1 binds C-terminus of all three VPs (only accessible when capsid has been denatured), and α-taxol binds to taxol. The AAV–taxol after dialysis sample shows robust A20 and taxol signals, indicating the virus capsids are intact and conjugated with taxol. Unconjugated AAV nanoparticles are detected by A20 but not by any of the other antibodies, indicating the capsids are intact and do not have any associated taxol. Free taxol-NHS dialyzed against 50% acetone in DPBS is included as a control to show our dialysis method effectively removes free taxol. Unconjugated AAV denatured via heat treatment at 75 °C and PBS only samples are included as controls for the AAV antibodies. Taxol-NHS only sample is included as a positive control for the α-taxol antibody.

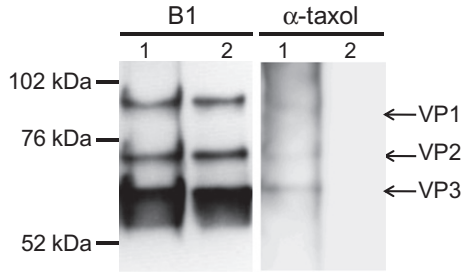

Fig. 4. Western blot of AAV–taxol conjugates show successful conjugation of taxol to VP subunits. B1 antibody binds to the C-terminus of all three capsid proteins and α-taxol antibody binds to taxol. Lane 1: AAV–taxol conjugate. Lane 2: wtAAV.

Capsid integrity of the AAV–taxol conjugation was further confirmed by TEM. Fig. 5 displays wtAAV (left panel) and AAV–taxol (right panel) virus images. We observe similar capsid morphologies in both samples, supporting the structural integrity of the conjugated virus. Overall, we have demonstrated successful conjugation of taxol onto AAV capsids and the resulting conjugates being structurally intact.

3.4. Conjugation does not negatively impact gene delivery or cytotoxicity of virus nanoparticles

We next evaluated if the conjugation reaction affected the functional properties of AAV. First, the ability of AAV–taxol to deliver genes to cells was tested via a transduction assay. Unconjugated and conjugated virus nanoparticles were added to HeLa cervical cancer cells and imaged for GFP transgene expression 48 h later (Fig. 6A). No difference in gene expression is observed between the two samples, indicating the conjugation reaction did not negatively impact the ability of AAV to deliver genes. Next, the cytotoxicity of virus nanoparticles was tested via a MTT assay. Unconjugated and conjugated virus nanoparticles were added to HeLa cervical cancer cells and probed for metabolic activity 72 h later (Fig. 6B). No difference in viability is observed between the two samples, indicating the conjugation of taxol onto the virus capsid did not impact the cytotoxicity of AAV. Overall, conjugation of tax-

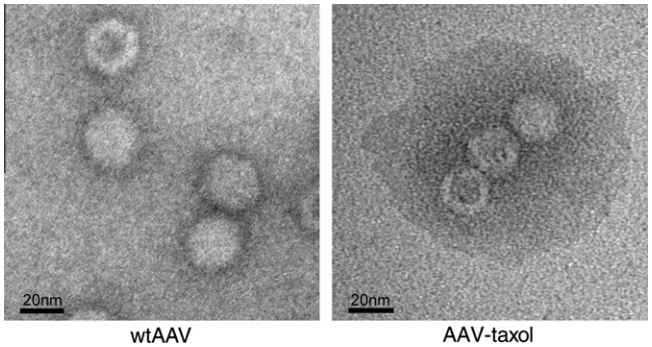

Fig. 5. TEM images of wtAAV (left) and AAV–taxol (right). Both samples were negatively stained with fresh 0.75% uranyl formate solution. We observe full capsids (light center) and empty capsids (dark center) for both samples.

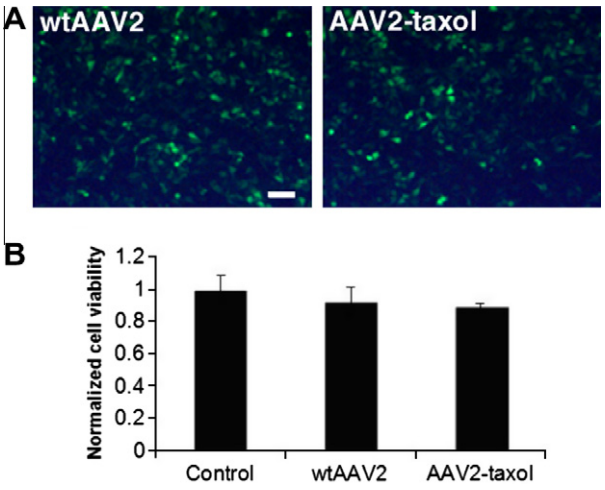

Fig. 6. Taxol conjugation to AAV nanoparticles does not negatively affect gene delivery efficiency or cell viability. (A) Virus nanoparticles, unconjugated or conjugated with taxol, were added to HeLa cells at an MOI of 10,000. At 48 h post-addition, GFP expression was imaged using fluorescence microscopy. Scale bar is 100 μm. Images are representative of three independent experiments. (B) Cytotoxicity of virus nanoparticles, unconjugated or conjugated with taxol, was tested via MTT viability assay. Virus nanoparticles were added to HeLa cells at an MOI of 50,000. At 72 h post-addition, metabolic activity of cells was measured using MTT. Data is normalized to the control samples.

ol on AAV does not appear to affect gene delivery efficiency or cytotoxicity of the virus nanoparticles.

3.5. Discussion

Due to low solubility issues, taxol is currently delivered clinically with the aid of chemical solvents. Unfortunately, solvents may lead to undesirable side effects. Conjugating taxol to delivery platforms, such as virus nanoparticles, should improve the solubility of the drug as well as enhance the therapeutic payload.

We have tested the ability of AAV nanoparticles to be chemically reacted with drug molecules. Our results indicate that the capsid is able to withstand the conjugation and purification conditions, which included dialysis against 50% acetone in DPBS (Figs. 3 and S3). Our immunoblotting results show successful conjugation of taxol to the virus capsid (Figs. 3 and 4). Furthermore, the conjugation process does not negatively impact gene delivery efficiency or cytotoxicity properties of the AAV capsid (Fig. 6), supporting future attempts at conjugating drugs to the virus.

During the course of our work, we were met with several challenges. The most considerable challenge was the difficulty in obtaining large quantities of virus material through the common virus preparation protocol involving the transfection of HEK293T producer cells. An average virus preparation yields approximately 1.5 mL of 5×10^{11}–1×10^{12} genomes/mL after iodixanol separation and heparin affinity column purification. This low amount of virus starting material precluded us from analyzing our conjugations via mass spectrometry (MS). We attempted both electrospray ionization (ESI) and matrix-assisted laser desorption/ionization time-of-flight (MALDI-TOF) MS but were unsuccessful at obtaining high quality signals. Therefore, any sort of quantification of conjugation was prevented. We were, however, able to detect successful taxol conjugation via dot blot and Western blot using the anti-taxol antibody. Unfortunately, no shifting of the VP bands were visible, perhaps reflecting low numbers of taxol molecules per subunit.

Moreover, the co-delivery of AAV and taxol to HeLa cells did not result in decreased viability of the cells as expected. MOIs up to 200,000 were tested, resulting in robust gene expression but no effect on cell viability (data not shown). Since we were unable to quantify the amount of taxol conjugated per virus capsid, our experimental limit was based on virus MOI that is reasonable to use in cell studies. This negative result can be due to a couple of factors. First, again, since we do not know quantitatively how much taxol we are delivering with each virus nanoparticle, we may be well below the LD50 of taxol in our cell study. Alternatively, the conjugated taxol may experience difficulty in releasing from the virus nanoparticle. Although the previous work using MS2 capsid utilized a similar ester bond for release of taxol, it may be that in the context of our virus platform the cleavage is not as efficient.

For future attempts to conjugate drugs to the AAV capsid, several improvements should be considered. First, the virus should be produced via a high-yield method, such as by using the baculovirus system (Aslanidi et al., 2009; Kotin, 2011; Negrete and Kotin, 2008a,b; Urabe et al., 2002). The typical yield of such production methods is reported to be 1L of 1×10^{14} vector particles. With the greater amount of virus material in hand, MS analysis of the conjugations will be more easily obtainable. This quantitative information will be critical in determining the efficacy of the drug-virus nanoparticle designs. Second, other types of cleavable linkers can be tested. For example, hydrazone linkers are highly acid-labile and have been shown to be effective at releasing drugs in cellular endosomes (Brunel et al., 2010; Dirksen and Dawson, 2008). With improvements in AAV–taxol production, we will be able to quantify drug loading, drug release, as well as in vivo efficacy and immunogenicity.

Overall, although we were unable to show effective killing of cancer cells using our virus-taxol nanoparticles, we have learned important lessons that can be used in future attempts at conjugating drugs to AAV. With improvements in virus source and possible alternatives in linker choice, we are optimistic of the AAV capsid being able to withstand the conjugation reaction conditions required to attach taxol, or other types of hydrophobic drugs, for co-delivery of drugs and genes.

Acknowledgments

The authors would like to thank Vamseedhar Rayaprolu and Brian Bothner for help with ESI mass spectrometry analysis. The work was supported by the Department of Defense Breast Cancer Research Program (BC087034).

Appendix A. Supplementary data

Supplementary data associated with this article can be found, in the online version, at doi:10.1016/j.ejps.2012.02.022.

References

Aslanidi, G., Lamb, K., Zolotukhin, S., 2009. An inducible system for highly efficient production of recombinant adeno-associated virus (rAAV) vectors in insect Sf9 cells. Proc. Natl. Acad. Sci. USA 106, 5059–5064.

Brunel, F.M., Lewis, J.D., Destito, G., Steinmetz, N.F., Manchester, M., Stuhlmann, H., Dawson, P.E., 2010. Hydrazone ligation strategy to assemble multifunctional viral nanoparticles for cell imaging and tumor targeting. Nano Lett. 10, 1093–1097.

Deutsch, H.M., Glinski, J.A., Hernandez, M., Haugwitz, R.D., Narayanan, V.L., Suffness, M., Zalkow, L.H., 1989. Synthesis of congeners and prodrugs. 3. Water-soluble prodrugs of taxol with potent antitumor activity. J. Med. Chem. 32, 788–792.

Dirksen, A., Dawson, P.E., 2008. Rapid oxime and hydrazone ligations with aromatic aldehydes for biomolecular labeling. Bioconjug. Chem. 19, 2543–2548.

Dosio, F., Brusa, P., Crosasso, P., Arpicco, S., Cattel, L., 1997. Preparation, characterization and properties in vitro and in vivo of a paclitaxel-albumin conjugate. J. Control. Release 47, 293–304.

Franzen, S., Lommel, S.A., 2009. Targeting cancer with 'smart bombs': equipping plant virus nanoparticles for a 'seek and destroy' mission. Nanomedicine (London, England) 4, 575–588.

Grieger, J.C., Samulski, R.J., 2005. Adeno-associated virus as a gene therapy vector: vector development, production and clinical applications. Adv. Biochem. Eng./Biotechnol. 99, 119–145.

Hillgenberg, M., Schlehofer, J.R., Von Knebel Doeberitz, M., Klein-Bauernschmitt, P., 1999. Enhanced sensitivity of small cell lung cancer cell lines to cisplatin and etoposide after infection with adeno-associated virus type 2. Eur. J. Cancer 35, 106–110.

Hughes, G.A., 2005. Nanostructure-mediated drug delivery. Nanomedicine 1, 22–30.

Jiang, M., Liu, Z., Xiang, Y., Ma, H., Liu, S., Liu, Y., Zheng, D., 2011. Synergistic antitumor effect of AAV-mediated TRAIL expression combined with cisplatin on head and neck squamous cell carcinoma. BMC Cancer 11, 54.

Koppold, B., Sauer, G., Buening, H., Hallek, M., Kreienberg, R., Deissler, H., Kurzeder, C., 2006. Chemotherapeutic agents enhance AAV2-mediated gene transfer into breast cancer cells promoting CD40 ligand-based immunotherapy. J. Cancer Res. Clin. Oncol. 132, 787–794.

Kotin, R.M., 2011. Large-scale recombinant adeno-associated virus production. Hum. Mol. Genet. 20, R2–R6.

Lataste, H., Senilh, V., Wright, M., Guenard, D., Potier, P., 1984. Relationships between the structures of taxol and baccatin III derivatives and their in vitro action on the disassembly of mammalian brain and Physarum amebal microtubules. Proc. Natl. Acad. Sci. USA 81, 4090–4094.

Loo, L., Guenther, R.H., Lommel, S.A., Franzen, S., 2008. Infusion of dye molecules into Red clover necrotic mosaic virus. Chem. Commun. (Cambridge, UK), 88–90.

Luo, Y., Prestwich, G.D., 1999. Synthesis and selective cytotoxicity of a hyaluronic acid-antitumor bioconjugate. Bioconjug. Chem. 10, 755–763.

Luo, Y., Ziebell, M.R., Prestwich, G.D., 2000. A hyaluronic acid-taxol antitumor bioconjugate targeted to cancer cells. Biomacromolecules 1, 208–218.

Magri, N.F., Kingston, D.G.I., 1986. Modified taxols. 2. Oxidation products of taxol. J. Org. Chem. 51, 797–802.

Manchester, M., Singh, P., 2006. Virus-based nanoparticles (VNPs): platform technologies for diagnostic imaging. Adv. Drug Deliv. Rev. 58, 1505–1522.

Mathew, A.E., Mejillano, M.R., Nath, J.P., Himes, R.H., Stella, V.J., 1992. Synthesis and evaluation of some water-soluble prodrugs and derivatives of taxol with antitumor activity. J. Med. Chem. 35, 145–151.

Mueller, C., Flotte, T.R., 2008. Clinical gene therapy using recombinant adeno-associated virus vectors. Gene Ther. 15, 858–863.

Musick, M.A., McConnell, K.I., Lue, J.K., Wei, F., Chen, C., Suh, J., 2011. Reprogramming virus nanoparticles to bind metal ions upon activation with heat. Biomacromolecules 12, 2153–2158.

Negrete, A., Kotin, R.M., 2008a. Large-scale production of recombinant adeno-associated viral vectors. Methods Mol. Biol. (Totowa, NJ, US) 433, 79–95.

Negrete, A., Kotin, R.M., 2008b. Strategies for manufacturing recombinant adeno-associated virus vectors for gene therapy applications exploiting baculovirus technology. Brief. Funct. Genomic. Proteomic. 7, 303–311.

Ogura, H., Nagai, S., Takeda, K., 1980. A novel reagent (N-succinimidyl diphenylphosphate) for synthesis of active ester and peptide. Tetrahedron Lett. 21, 1467–1468.

Parness, J., Kingston, D.G.I., Powell, R.G., Harracksingh, C., Horwitz, S.B., 1982. Structure-activity study of cytotoxicity and microtubule assembly in vitro by taxol and related taxanes. Biochem. Biophys. Res. Commun. 105, 1082–1089.

Ren, Y., Wong, S.M., Lim, L.-Y., 2007. Folic acid-conjugated protein cages of a plant virus: a novel delivery platform for doxorubicin. Bioconjug. Chem. 18, 836–843.

Steinmetz, N.F., 2010. Viral nanoparticles as platforms for next-generation therapeutics and imaging devices. Nanomedicine 6, 634–641.

Urabe, M., Ding, C., Kotin, R.M., 2002. Insect cells as a factory to produce adeno-associated virus type 2 vectors. Hum. Gene Ther. 13, 1935–1943.

Wu, W., Hsiao, S.C., Carrico, Z.M., Francis, M.B., 2009. Genome-free viral capsids as multivalent carriers for taxol delivery. Angew. Chem. Int. Ed. 48, 9493–9497, S9493/9491–S9493/9412.

Xiao, X., Li, J., Samulski, R.J., 1998. Production of high-titer recombinant adeno-associated virus vectors in the absence of helper adenovirus. J. Virol. 72, 2224–2232.

Yoo, J.-W., Irvine, D.J., Discher, D.E., Mitragotri, S., 2011. Bio-inspired, bioengineered and biomimetic drug delivery carriers. Nat. Rev. Drug Discov. 10, 521–535.

Zhang, K., Jiao, X., Liu, X., Zhang, B., Wang, J., Wang, Q., Tao, Y., Zhang, D., 2010. Knockdown of snail sensitizes pancreatic cancer cells to chemotherapeutic agents and irradiation. Int. J. Mol. Sci. 11, 4891–4904.